

Transient polarization dynamics in a CO₂ laser

I. Leyva^{1,2,*}, E. Allaria¹, and R. Meucci¹

¹ *Istituto Nazionale di Ottica Applicata,*

Largo E. Fermi 6, 50125 Florence, Italy and

² *Universidad Rey Juan Carlos. c/Tulipan s/n. 28933 Mostoles Madrid, Spain*

Abstract

We study experimentally and theoretically the polarization alternation during the switch-on transient of a quasi-isotropic CO₂ laser emitting on the fundamental mode. The observed transient dynamics is well reproduced by means of a model which provides a quantitative discrimination between the intrinsic asymmetry due to the kinetic coupling of molecules with different angular momenta, and the extrinsic anisotropies, due to a tilted intracavity window. Furthermore, the experiment provides a numerical assignment for the decay rate of the coherence term for a CO₂ laser.

PACS numbers:

*Electronic address: ileyva@ino.it

I. INTRODUCTION

Laser dynamics is commonly studied considering the electric field as a scalar variable, since in most systems the polarization state is imposed by anisotropies of the cavity. For instance, Brewster windows or gratings, generally used in gas lasers to close the laser tube or to select a vibro-rotational transition, impose a linearly polarized state of the laser emission. However, in perfectly cylindrical laser cavities without any elements to select a preferred polarization, the study of the dynamics includes the necessity of considering the vector nature of the electric field.

Several theoretical works have been devoted to the study of the polarization dynamics of the quasi-isotropic laser, showing the important role played by the material variables. In particular, the degeneracy of the angular momentum states of the laser transition sublevels has been considered as the coupling source between different polarization states. Initial studies considered only stationary solutions [1, 2], but more recently dynamical models have been developed to explore the role of anisotropy due to the laser medium, that from now on we will call intrinsic anisotropy [3, 4, 5, 6]. These models predict a rich dynamics even for the simplest transition, $J = 1 \rightarrow J = 0$. Later versions of these models include also linear and circular cavity anisotropies that we call extrinsic [8, 9], or different level structure [10].

However, up to now few experiments have been performed on this subject. Experiments carried out on noble gas lasers reveal that in some systems it is necessary to consider the dynamics of the matter variables to fully understand the polarization features of an isotropic system [2, 11]. In other cases, the observations could be explained by a nonlinear coupling of the modes and residual cavity anisotropies [13, 14].

In this work we present experimental and theoretical results for the polarization competition dynamics in the transient state of a quasi-isotropic low-pressure CO₂ laser. We show that the polarization dynamics during the switch-on is well described by means of a model including optical coherences (intrinsic anisotropy) and extrinsic linear anisotropies. These results extend our previous work in which the coherences were simplified as a parametric cross coupling between the matter polarization and electric fields [15], and provide a quantitative comparison between the amount of anisotropy due to the coupling of molecular angular momenta and that induced by an intracavity window. Furthermore, the decay rate of the coherences, defined in Ref. [3], is shown explicitly to be closer to the decay rate of

the population inversion rather than to the decay rate of the induced polarization.

II. EXPERIMENTAL RESULTS

The experiment has been performed using an unpolarized Fabry-Perot cavity as shown in Fig. 1. A total reflective flat mirror (M_1 , reflectivity $R_1=1$) and an outcoupler mirror (M_2) with a reflectivity $R_2 = 0.914$ set the cavity length at $L = 75$ cm. A piezo translator (Pzt) is used to select the P(20) laser emission line and to adjust the laser detuning.

The active medium, a mixture of He (82%), N_2 (13.5%) and CO_2 (4.5%) at a pressure of 25 mbar, is pumped by a DC discharge fixed at 6.1 mA when the threshold current is 3 mA.

As we are interested in the transient dynamics, an intracavity chopper is used to induce a switch-on event at a repetition rate of 200 Hz.

In order to control the linear anisotropies of the cavity, a ZnSe anti reflection coated window (W) has been introduced, which can be tilted accurately as shown in Fig.1.

The polarization state of the laser emission has been analyzed by means of a wire grid polarizer (Pol), which has the property of reflecting one linear polarization of the incident radiation and transmitting the orthogonal one, with an extinction ratio of 1:180. The reflected and transmitted parts of the beam are directed to two HgCdTe fast detectors (D_1 , D_2 , 100 MHz bandwidth), whose sensitive areas ($10^4 \mu m^2$) are much smaller than the beam size. Both signals are recorded on a digital oscilloscope (Lecroy LT423L) with 500 MHz bandwidth.

In the stationary regime, we observe that the laser has two possible linear polarization directions which are orthogonal as far as we can measure. In Fig. 1 these cavity eigendirections are called H and V respectively.

The window W can rotate by an angle θ around the axis V. When $\theta = 0$, the polarization direction is determined by the detuning of the cavity, as usual [2, 8, 16]. This is illustrated in Fig.2(a), where we plot the laser intensity along both eigendirections when the detuning is varied around the line center. A residual hysteresis around the transition is masked by the limited resolution of Pzt. At the transition point near the line center there is not a preferred polarization direction and the laser flips spontaneously from one to other as shown in Fig. 3.

Our goal is to study the polarization behavior in this bistable region. In particular, we analyze of the switch-on transient state, in which the total intensity presents relaxation oscillations. In our system the pump strength imposes a relaxation frequency of 55 KHz.

When the two polarized components are separated, they show oscillations in relative antiphase, which do not appear on the total intensity (Fig.4). The amplitude of these oscillations depends on the angle between the polarizer axes with respect to H-V, reaching a maximum when the analysis is performed at 45° .

In Fig.4(a) we report an example of these polarization oscillations, when the cavity is tuned at the center of the line. The total laser output intensity (thick solid line) is displayed together with its two orthogonally polarized components analyzed at 45° (thin solid and dashed lines).

These oscillations are always damped until they disappear, with a damping rate depending on the cavity detuning. Precisely the oscillations are more persistent the closer is the detuning to the bistable region. This fact points to the competitive origin of the oscillations. In Fig.4 (c) we show an example of the transient dynamics when the cavity detuning is slightly moved from resonance. It is worth to note that the system is so sensible to noise that the duration of the oscillations suffers slight variations, without apparent changes in the conditions.

Successively, we studied the response of the system to small linear anisotropies driven by the tilt angle θ of the intracavity window W around the vertical axis.

Several parameters of the system are simultaneously affected by this action. As a consequence of the common increasing of the optical path for both polarization eigendirections, the line center moves with respect to the isotropic condition $\theta = 0$. In order to keep the bistable condition, the cavity length is varied to recover the resonance.

In Fig.2((b) and (c)) we show the intensity of both polarization components for different θ values, showing that the gain profile is not significantly distorted with respect to the isotropic condition $\theta = 0$ (Fig.2(a)). The detuning anisotropies are measured to be smaller than 5% of the total change.

The other effect of the tilt angle θ is to increase the cavity losses. In Fig.6 (b) we report the dependence of the laser intensity on the tilt angle θ which is in agreement with the expected theoretical behavior [7]. Moreover, since the gain profiles for the two polarization directions do not change due to the tilt angle θ (Fig. 2), we can assume that the induced

loss anisotropies remain a small effect ($\simeq 1\%$) compared to the total loss change. The effect of the losses anisotropy can be observed in the residual modulation in the total intensity (Figs.4 (a),(c)).

The dynamical effect observed when θ is increased is the growing of the frequency of the polarization oscillations. Measurements made near the resonance condition show that the frequency rises as the tilt angle increased (Fig.6 (a)). It can be seen that a tilt angle of 12° is enough to rise the frequency from 100 KHz to 400 KHz.

III. MODEL AND NUMERICAL RESULTS

Our theoretical approach is based on the theory of the isotropic laser developed in Ref. [3] where the optical coherences between upper levels are considered with the. This theory was developed for the simplest case ($J=1 \rightarrow J=0$), while the transition involved in our system is much more complicated ($J=19 \rightarrow J=20$). However, this theory has been showed to predict also the behavior of lasers with a different level structure, as shown in Ref. [11]. Only first order coherences ($\Delta m = \pm 1$) will be considered. Therefore, independently of the number of sublevels, there are only two kind of possible transitions, which generate a split of the population in two ensembles, in such a way that an anisotropy is induced in the active medium [6]. Furthermore we introduce an extrinsic linear anisotropy as done in Ref.[8].

The field will be decomposed in a circularly polarized base. Just losses and linear de-tuning anisotropies along the principal axes of the system will be included, but not circular asymmetries since our system does not show signs of dicroism. It reads as

$$\begin{aligned}
\dot{E}_R &= \kappa(P_R - E_R) + i\delta E_R - (\alpha + i\beta)E_L, \\
\dot{E}_L &= \kappa(P_L - E_L) + i\delta E_L - (\alpha + i\beta)E_R, \\
\dot{P}_R &= -\gamma_\perp[P_R - D_R E_R - E_L C], \\
\dot{P}_L &= -\gamma_\perp[P_L - D_L E_L - E_R C^*], \\
\dot{C} &= -\gamma_c C - \frac{\gamma_\parallel}{4}(E_L^* P_R + E_R P_L^*), \\
\dot{D}_R &= -\gamma_\parallel[D_R - r + \frac{1}{2}(E_R P_R^* + E_R^* P_R) + \frac{1}{4}(E_L P_L^* + E_L^* P_L)], \\
\dot{D}_L &= -\gamma_\parallel[D_L - r + \frac{1}{2}(E_L P_L^* + E_L^* P_L) + \frac{1}{4}(E_R P_R^* + E_R^* P_R)]
\end{aligned} \tag{1}$$

where $E_R(\vec{r}, t), E_L(\vec{r}, t)$ are the slowly varying electric fields in the circular basis.

$P_R(\vec{r}, t)$, $P_L(\vec{r}, t)$ stand for the matter polarization fields, $D_R(\vec{r}, t)$ and $D_L(\vec{r}, t)$ are the respective population inversions. The field $C(\vec{r}, t)$ represents the coherence between the upper sublevels. We recall that, in a density matrix treatment, the polarization correspond to off diagonal matrix elements between upper and lower level of the radiative transition, whereas C is proportional to the of diagonal matrix elements coupling different angular momentum states of the upper level [11]. The parameter δ represents the detuning between the cavity and the atomic transition frequencies. The parameters $\alpha = (\kappa_V - \kappa_H)/2$ and $\beta = (\delta_H - \delta_V)/2$ represent respectively the linear anisotropies in the losses and detuning with respect to the cavity H-V axes, where κ_V , κ_H , are the losses in the horizontal and vertical axis, and δ_V , δ_H are the corresponding detunings.

In our low pressure CO₂ laser, the polarization decay is $\gamma_\perp = 4.4 \cdot 10^8 \text{ s}^{-1}$ and the inversion decay rate as $\gamma_\parallel = 1.95 \cdot 10^5 \text{ s}^{-1}$ [15]. In view of numerical solutions, there is no reason to keep dynamical equations for variables whose decay rates differ by several orders of magnitude. Depending on whether $\gamma_c \simeq \gamma_\parallel$ or $\gamma_c \gg \gamma_\parallel$, we can respectively reduce the number of differential equations from 7 to 5 (for E_R , E_L , C , D_R and D_L) or 4 (for E_R , E_L , D_R and D_L). In the first case, P_R , P_L are eliminated adiabatically and their values correspond to the stationary solutions of the third and fourth of Eqs. 1. In the second case (fast C), also the C variable is eliminated adiabatically and it follows the relatively slow variations of the field and the population inversion. Whether to choose between five or four equations depends on the numerical value of γ_c . The γ_c parameter represents the coherence decay rate, whose value should be chosen between γ_\perp and γ_\parallel [5]. However, this parameter can not be directly measured, and it will be used as control parameter in order to fit the theory to the experimental results [8]. We find that the optimal value is $\gamma_c \simeq \gamma_\parallel$ in all cases, which is also consistent with the observation that just linearly polarized states are found in the experiment. Indeed, a higher value of γ_c would give rise to a periodic modulation of the total intensity [5] which has never been observed in our experiments. Hence, the coherence C decays on the same time scale as the population inversion and we must keep the corresponding time dependent equation. Thus our experimental system is dynamically modeled as a class B laser [12], and Eqs. (1) reduce to the following system of two algebraic

equations:

$$\begin{aligned} P_R &= D_R E_R + E_L C \\ P_L &= D_L E_L + E_R C^* \end{aligned} \quad (2)$$

and five differential equations:

$$\begin{aligned} \dot{E}_R &= \kappa(D_R - 1)E_R + i\delta E_R + (\kappa C - (\alpha + i\beta)) E_L, \\ \dot{E}_L &= \kappa(D_L - 1)E_L + i\delta E_L + (\kappa C^* - (\alpha + i\beta)) E_R, \\ \dot{C} &= -\gamma_{\parallel}(C(1 + \frac{1}{4}(|E_L|^2 + |E_R|^2)) - \frac{1}{4}E_R E_L^*(D_L + D_R)), \\ \dot{D}_R &= -\gamma_{\parallel} \left[D_R(1 + |E_R|^2) - r + \frac{1}{2} \left(D_L |E_L|^2 + \frac{3}{2}(E_R E_L^* C^* + E_R^* E_L C) \right) \right], \\ \dot{D}_L &= -\gamma_{\parallel} \left[D_L(1 + |E_L|^2) - r + \frac{1}{2} \left(D_R |E_R|^2 + \frac{3}{2}(E_R E_L^* C^* + E_R^* E_L C) \right) \right]. \end{aligned} \quad (3)$$

Eqs. (3) show explicitly that the cross field coupling is due partly to a molecular coupling $J = 1 \rightarrow J = 0$ (intrinsic) and partly to the intracavity window W (extrinsic). Fig. 5 provides evidence that the main responsible for the alternation is the intrinsic anisotropy rather than the extrinsic one. Figure 5 (a) refers to the case where both coherences and linear anisotropies are acting. In Fig. 5 (b), the extrinsic anisotropy has been removed. now the oscillation competition is not damped, but the alternation of the two polarization is maintained. Finally, in Fig. 5 (c) just the extrinsic anisotropies are acting; the competition does not appear any more.

From the experimental observations we know that the most important effect of the window tilting is the increase of the total loss, while the losses and detuning anisotropies represent a minor effect. In addition, as the excitation current does not change during the experiment, the increasing of the losses affects the gain to loss ratio. As a consequence, the total losses κ and pump parameter r are functions of θ as follows [7]:

$$r(\theta) = r_o(1 - a_r \sin(\theta)^4) \quad (4)$$

$$\kappa(\theta) = \kappa_o(1 + a_k \sin(\theta)^4) \quad (5)$$

where $r_o = 2$ and $\kappa_o = -\frac{c}{4L} \log(R) = 4.1 \cdot 10^6 \text{ s}^{-1}$ are the pump strength and total losses when the tilt angle $\theta = 0$. Here c is the speed of light, $L = 0.75 \text{ m}$ the cavity length and $R = \sqrt{R_1 R_2} = 0.956$ the mirrors reflectivity. the parameters $a_r = 150$ and $a_k = 25000$ are related to the reflectivity of the window W, and are chosen to fit the experimental results.

In Fig. 4 (b) and (d) the numerically generated intensity profiles are compared with their experimental counterparts reported in Fig 4 (a) and (c), respectively. It can be observed that the intensity profiles show antiphase oscillations for both polarization components, while the total intensity remains unmodulated.

When $\delta=0$, the polarization oscillations remain undamped for any degree of anisotropy. For $\delta \neq 0$, the oscillations are still undamped only in perfect cavity symmetry conditions $\alpha = \beta = 0$. In Fig.4 (d) it can be seen that for $\delta = 0.05$, a detuning or losses anisotropy of 0.5 % is sufficient to damp the oscillation in a few hundred microseconds as observed in the experiment. In the experimental system unavoidable residual anisotropies break the cylindrical symmetry, and therefore the polarization oscillations are always damped.

Choosing the resonant condition $\delta = 0$, we observe that the frequency of the oscillations presents the same dependence on the total losses and pump strength found in the experiment. In Fig. 6 we compare the experimental and numerical angular dependences of the polarization oscillation frequency (Fig. 6 (a),(c)) and the total intensity (Fig. 6 (b),(d)), showing good agreements.

IV. CONCLUSIONS

In this work we have reported an experimental and theoretical study of the transient polarization dynamics of a quasi-isotropic CO₂ laser. A competition between two modes with orthogonal polarization directions is observed. The competition manifests itself as an oscillation on the polarized laser field, whose features depend on the cavity parameters.

To explain the observed transient polarization alternation, both intrinsic and extrinsic anisotropies must be considered; the intrinsic ones provide the alternation and the extrinsic ones provide damping and residual ripple of the total intensity. The numerical results fit well with the experimental observations, pointing out the importance of matter variables in the dynamics of a quasi-isotropic laser.

The authors are grateful to F.T. Arecchi for fruitful discussions.

[1] M. Sargent and W. E. Lamb. Phys. Rev **164**, 436 (1967).

- [2] D. S. Bakaev, V. M. Ermachenko, V. Yu Kurochin, V. N. Petrovshil, E. D. Protsenko, A. N. Rurukin and Shanenin. Sov. J. Quantum. Electron **18**, 1 (1988).
- [3] G. C. Puccioni, M. V. Trantnik, J.E. Sipe and G. L. Oppo Opt. Lett. **12**, (1987).
- [4] N. B. Abraham, E. Arimondo, M. San Miguel. Optics Comm. **117**, 344 (1995).
- [5] N. B. Abraham, M. D. Matlin and R. S. Gioggia. Phys. Rev. A **53**, 3514 (1996).
- [6] For a review see: G. M. Stephan and A. D. May. Quantum Semiclass. Opt. **10**, 19 (1998).
- [7] *Principles of Optics*. M. Born and E. Wolf. 6th edition. Cambridge University Press (1980).
- [8] M. D. Matlin, R. S. Gioggia, N. B. Abraham, P. Glorieux and T. Crawford Opt. Comm. **120**, 204 (1995).
- [9] J. Redondo, G. J. de Varcárcel and E. Roldán. Phys. Rev. A **56**, 648 (1997).
- [10] A. Kulminskii, R. Vilaseca, R. Corbalan and N. B. Abraham, Phys. Rev. A **62**, 648 (2000).
- [11] G. C. Puccioni, G. L. Lippi and N. B. Abraham. Optics Comm. **72**, 361 (1989).
- [12] F.T. Arecchi in *Instabilities and chaos in quantum optics*, (Eds. F.T. Arecchi and R.G. Harrison), Springer Series Synergetics, Vol. 34 pp. 9-48 (1987).
- [13] C. Taggiasco, R. Meucci, M. Ciofini and N. B. Abraham. Optics Comm. **133**, 507 (1997).
- [14] A. Labate, R. Meucci, M. Ciofini, N. B. Abraham and C. Taggiasco. Quantum Semiclass. Opt. **10**, 115 (1998).
- [15] I. Leyva, E. Allaria and R. Meucci. Optics Lett. **26**, 605 (2001).
- [16] M. A. van Eijkelenborg, C. A. Schrama and J. P. Woerdman. Optics Comm. **119**, 97 (1995).

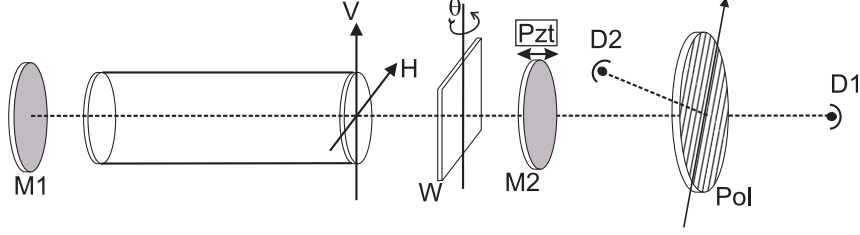


FIG. 1: Experimental setup: M_1 : total reflecting flat mirror, W : additional intracavity window, M_2 : outcoupler mirror, V : Vertical axis of the cavity, H : Horizontal axis of the cavity, Pzt : piezo electro translator, Pol : wire grid polarizer, D_1 : fast detector for the vertical component, D_2 : fast detector for the horizontal component

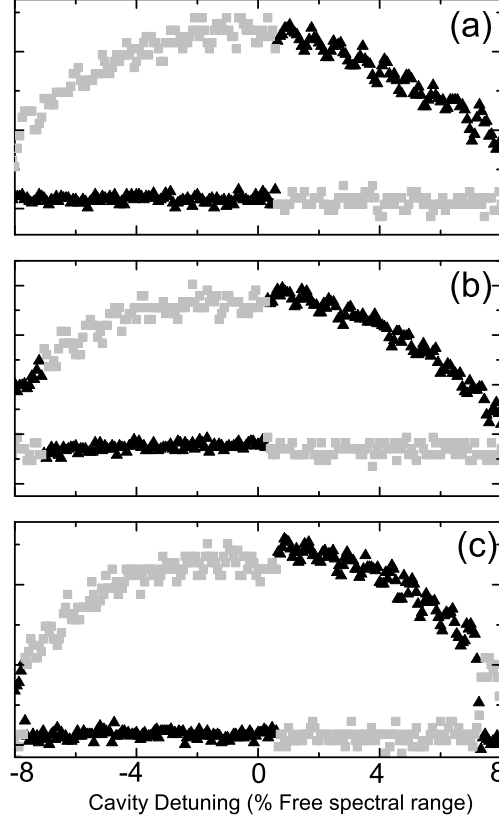


FIG. 2: Experimental intensity of both polarization components along a free spectral range (Black triangles vertical polarization direction, gray squares horizontal polarization direction) (a) quasi isotropic condition $\theta = 0$ (b) $\theta = 6^\circ$ (c) $\theta = 9^\circ$. It is to be noted that a Pzt adjustment is required to recover the resonant condition for each θ .

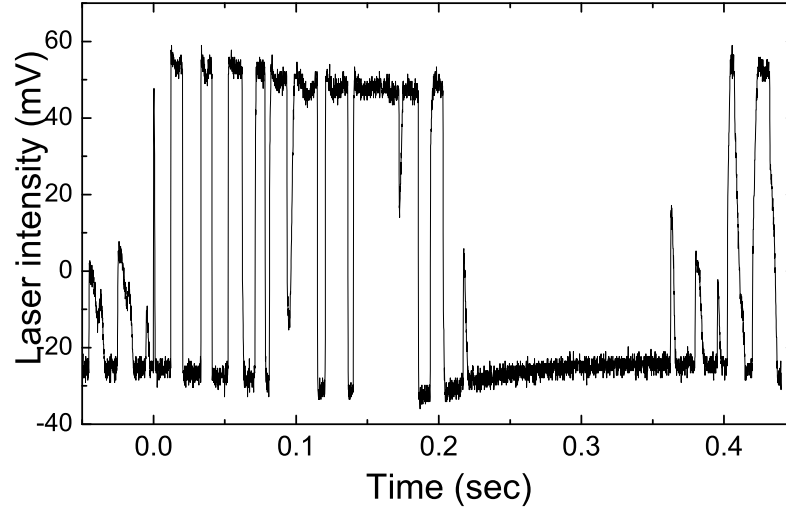


FIG. 3: Intensity of vertical polarization component when the cavity detuning is chosen at the transition point near the resonance.

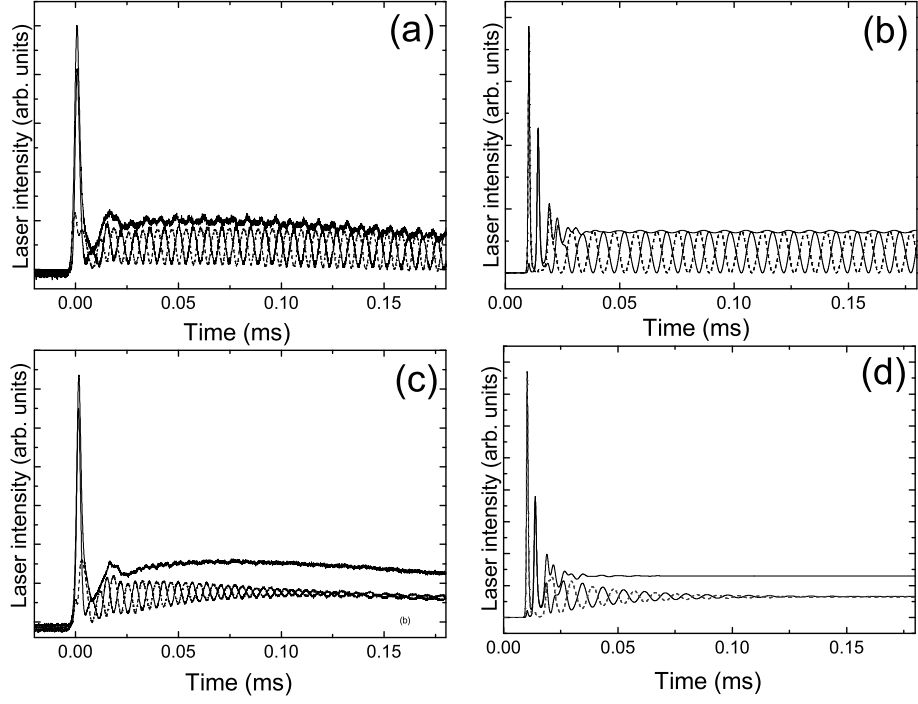


FIG. 4: Experimental time intensity profiles for $\theta = 0$ and slightly different detuning condition : (a) resonance, (c) out of resonance. Numerical generated intensity profiles for $\theta=0$, $\alpha = \beta = 0.01$ and : (b) $\delta = 0$, (d) $\delta = 0.05$.

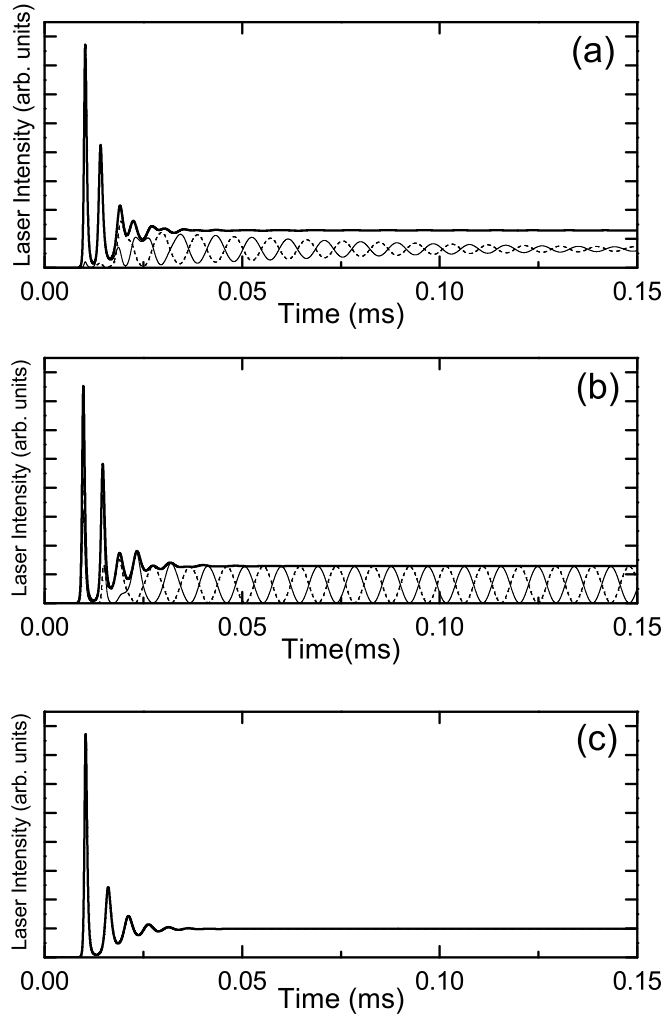


FIG. 5: Numerical intensity profiles for $\delta = 0.05$, $\theta=0$ and : (a) $\alpha = \beta=0.005$, (b) $\alpha = \beta=0.0$ and (c) $\alpha = \beta=0.005$, $C=0$.

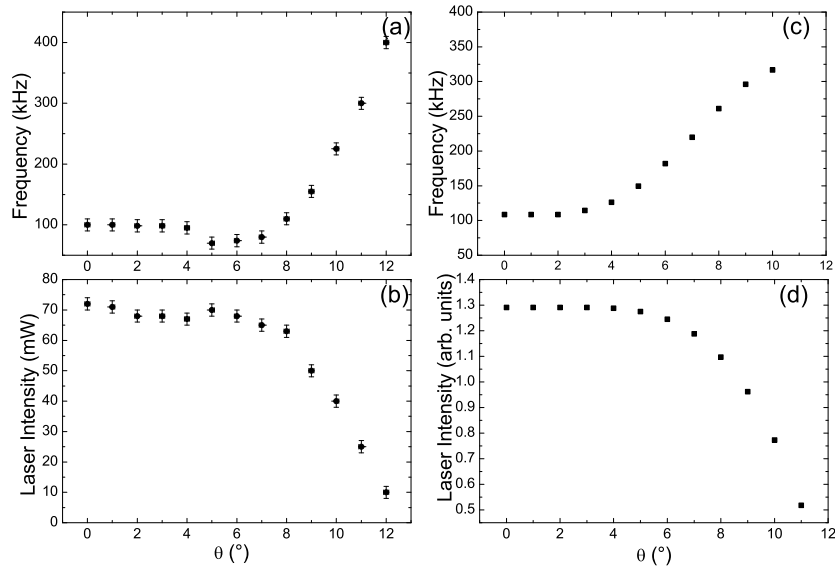


FIG. 6: Experimental angular dependences of: (a) polarization oscillation frequency and (b) total intensity. Numerical dependences ($\delta = 0$, $\alpha=0.01$ $\beta=0.01$): (c) polarization oscillation frequency and (d) total intensity.